Baghdad Science Journal

Volume 23 | Issue 1 Article 11

1-1-2026

Double-Layered Tin-Polydimethylsiloxane (PDMS) Composites: Evaluation of Porosity and Structural Morphology of Polymeric Composites

Nurul Syafiqah Roslan
Department of Applied Sciences, Universiti Teknologi MARA Cawangan Pulau Pinang, 13500 Permatang Pauh, Pulau Pinang, Malaysia, 2024592857@student.uitm.edu.my

Nur Maizatul Azra Mukhtar
Department of Applied Sciences, Universiti Teknologi MARA Cawangan Pulau Pinang, 13500 Permatang Pauh, Pulau Pinang, Malaysia; Faculty of Health Sciences, Universiti Teknologi MARA Cawangan Pulau Pinang,13200 Kepala Batas, Pulau Pinang, Malaysia AND Department of Biomedical Imaging, Advanced Medical and Dental Institute, Universiti Sains Malaysia, SAINS@BERTAM, 13200 Kepala Batas, Pulau Pinang, Malaysia, nurmaizatul038@uitm.edu.my

Ainorkhilah Mahmood
Department of Applied Sciences, Universiti Teknologi MARA Cawangan Pulau Pinang, 13500 Permatang Pauh, Pulau Pinang, Malaysia, ainorkhilah_sp@uitm.edu.my

Nor Aimi Abdul Wahab
Department of Applied Sciences, Universiti Teknologi MARA Cawangan Pulau Pinang, 13500 Permatang Pauh, Pulau Pinang, Malaysia, noraimi108@uitm.edu.my

Rafidah Zainon
Department of Biomedical Imaging, Advanced Medical and Dental Institute, Universiti Sains Malaysia, SAINS@BERTAM, 13200 Kepala Batas, Pulau Pinang, Malaysia, rafidahzainon@usm.my

How to Cite this Article

Roslan, Nurul Syafiqah; Mukhtar, Nur Maizatul Azra; Mahmood, Ainorkhilah; Wahab, Nor Aimi Abdul; Zainon, Rafidah; Abidin, Hanisah Zainal; Shah, Aishah Zarzali; and Izaham, Nor Iwani Nor (2026) "Double-Layered Tin-Polydimethylsiloxane (PDMS) Composites: Evaluation of Porosity and Structural Morphology of Polymeric Composites," *Baghdad Science Journal*: Vol. 23: Iss. 1, Article 11.
DOI: https://doi.org/10.21123/2411-7986.5141

See next page for additional authors

Double-Layered Tin-Polydimethylsiloxane (PDMS) Composites: Evaluation of Porosity and Structural Morphology of Polymeric Composites

Authors

Nurul Syafiqah Roslan, Nur Maizatul Azra Mukhtar, Ainorkhilah Mahmood, Nor Aimi Abdul Wahab, Rafidah Zainon, Hanisah Zainal Abidin, Aishah Zarzali Shah, and Nor Iwani Nor Izaham

BAGHDAD SCIENCE JOURNAL 2026;23(1):138–150

SPECIAL ISSUE ARTICLE

Double-Layered Tin-Polydimethylsiloxane (PDMS) Composites: Evaluation of Porosity and Structural Morphology of Polymeric Composites

Nurul Syafiqah Roslan [1], Nur Maizatul Azra Mukhtar [1,2,3,*], Ainorkhilah Mahmood [1], Nor Aimi Abdul Wahab [1], Rafidah Zainon [3], Hanisah Zainal Abidin [1], Nor Iwani Nor Izaham [4], Aishah Zarzali Shah [5]

[1] Department of Applied Sciences, Universiti Teknologi MARA Cawangan Pulau Pinang, 13500 Permatang Pauh, Pulau Pinang, Malaysia
[2] Faculty of Health Sciences, Universiti Teknologi MARA Cawangan Pulau Pinang,13200 Kepala Batas, Pulau Pinang, Malaysia
[3] Department of Biomedical Imaging, Advanced Medical and Dental Institute, Universiti Sains Malaysia, SAINS@BERTAM, 13200 Kepala Batas, Pulau Pinang, Malaysia
[4] Faculty of Applied Sciences, Universiti Teknologi MARA Shah Alam, 40450 Shah Alam, Selangor, Malaysia
[5] Centre of Foundation Studies UiTM, Universiti Teknologi MARA Cawangan Selangor, Kampus Dengkil, 43800 Dengkil, Selangor, Malaysia

ABSTRACT

The pursuit of advanced materials for radiation protection has highlighted the potential of polymer–metal composites. Porosity is a key factor influencing radiation attenuation, as fewer voids reduce pathways for radiation penetration. Recent studies emphasize the role of filler distribution in enhancing both mechanical properties and shielding performance. This work investigates the structural morphology and porosity of tin–PDMS composites prepared with pure tin (PS) and tin alloy (AS) fillers at 10–60 wt.% loadings, along with a tin–alloy mixture series (TM). Morphological features, particle distribution, oxygen content, and porosity were comprehensively analyzed. Results show that porosity strongly correlates with filler distribution and composition. The AS5 composite (50 wt.% tin alloy) exhibited the most balanced properties, achieving a low porosity of 0.34% with satisfactory density and microstructural stability. Within the TM series, TM6 (60 wt.% tin mixture) demonstrated promising features for high-density shielding applications due to its high tin content with a density of 5.32 g/cm^3 and porosity less than 2.0% of the nominal acceptance threshold for the composite. These findings establish the foundational microstructural characteristics of tin–PDMS composites as a step toward developing lead-free radiation shielding materials.

Keywords: Double-layer composite, ImageJ, Metal-polymer, Porosity, Radiation shielding

Introduction

Given their superior X-ray absorption, high atomic numbers of atoms like bismuth, tungsten, and tin have a high potential to replace lead in mitigating radiation exposure.[1] High-energy photons released by electromagnetic radiation emit a lot of energy. The photoelectric effect is one of the emission-related interactions. A core electron will be ejected from an irradiated substance if the photon energy surpasses the core electron's binding energy. Consequently, the photoelectric effect is more likely to occur in metals with greater atomic numbers. Metal-polymer composites for radiation shielding are often produced using low-density polymers such as PDMS as a matrix.[2] These materials are lead-free composites

Received 28 February 2025; revised 24 September 2025; accepted 30 September 2025.
Available online 1 January 2026

* Corresponding Author.
E-mail addresses: 2024592857@student.uitm.edu.my (N. Syafiqah Roslan), nurmaizatul038@uitm.edu.my (N. Maizatul Azra Mukhtar), ainorkhilah_sp@uitm.edu.my (A. Mahmood), noraimi108@uitm.edu.my (N. Aimi Abdul Wahab), rafidahzainon@usm.my (R. Zainon), 2023650308@student.uitm.edu.my (H. Zainal Abidin), 2023186261@student.uitm.edu.my (N. Iwani Nor Izaham), aishah.zarzali@uitm.edu.my (A. Zarzali Shah).

International Conference on Discoveries in Applied Sciences and Applied Technology (DASAT2025)
https://doi.org/10.21123/2411-7986.5141

that shield radiation and are lightweight, safe, and durable.[3,4] Silicon material can withstand radiation doses of up to 500 kGy and is resistant to radiation cross-linking, radiation-induced polymerization, and polymer breakdown.[5] Composite fabrication techniques affect how effectively radiation is absorbed. Not all materials are acceptable for manufacture, as evidenced by specific needs in the medical industry, such as PPE and radiation shielding construction.[6–8] For the radiation process to be protected, the composite structure needs to be sufficiently flexible and safe.[9] Additionally, the composite performance is impacted by homogeneity. The composite requires time to solidify if the mixture contains particles of varying sizes and shapes in the polymer matrix, and the high-density particles will settle to the bottom of the composite.[10] Thus, creating the composite in layers is an effective approach to address this issue.

More atoms per unit volume interact and absorb the radiation, and higher-density materials offer superior shielding.[11,12] Upgrading a single layer to several layers can tailor the composite density and shielding attenuation properties.[13] As each layer of the multilayer composite has a high-tolerance composition, the composite density rises. According to the literature, multilayered composites are still stages of development and have not yet been extensively investigated as a lead substitute for radiation shielding.[14–16] Thus, this research was carried out to develop a flexible, lead-free, multilayered PDMS composite by incorporating pure tin powders and tin alloys at a specific composition ratio.

Metal filler and polymer

The development of metal–polymer composites for radiation shielding is motivated by the need for safe, lead-free materials that balance shielding performance with mechanical flexibility.[17,18]. Tin-based composites, in particular, offer advantages such as lower toxicity, favorable density, and good chemical compatibility with polymer matrices. Studies have shown that tin–PDMS composites are promising for medical radiation shielding, as they reduce weight while maintaining shielding efficiency. Furthermore, investigations confirm their durability under prolonged radiation exposure.

Layered fabrication approaches enhance these benefits by introducing multiple interfaces that scatter and absorb radiation more effectively. Layering also improves mechanical durability, prevents filler sedimentation, and allows tailoring of shielding performance by controlling layer thickness and composition. These advantages highlight the versatility of tin–PDMS systems and underscore the importance of understanding how filler type, distribution, and porosity influence composite performance.

Porosity of the metal-polymer composite

Porosity significantly impacts the effectiveness of radiation shielding materials.[19–21] High-Z fillers such as tin, tungsten, or bismuth can enhance attenuation, but excessive porosity reduces density, weakens structural integrity, and creates channels through which radiation may pass. In high-precision applications such as medical devices, personal protective equipment, and aerospace components, porosity must be minimized to maintain reliability, durability, and protection efficiency.[22]

Conversely, carefully controlled porosity may sometimes be introduced for weight reduction or flexibility, though these compromises shielding efficiency. Therefore, quantifying and controlling porosity is critical to designing composites that balance mechanical properties and radiation attenuation. This study emphasizes porosity analysis as a central parameter in evaluating tin–PDMS composites, linking composition ratios with observed microstructural features. Reliability is of utmost importance in medical and aerospace applications, and these parameters can be deteriorated by porosity.[23]

Materials and methods

The raw materials used in this study consisted of metal powders and a polymer matrix. Pure tin (Sn) powder, with a density of approximately 7.31 g/cm^3, was obtained from Bendosen, Kuala Lumpur, Malaysia, while a tin alloy powder, with a density of about 8.8 g/cm^3, was supplied by Sigma Aldrich, Taufkirchen, Germany. Both pure tin and tin alloy powders were provided in micron-sized particulate form. The polymer matrix employed was polydimethylsiloxane (PDMS), purchased as the Sylgard 184 Silicone Elastomer Kit (Dow Corning, USA), which included both the PDMS elastomer base and the corresponding curing agent. As for the first layer, the tin and PDMS were mixed and stirred for about 7 to 10 minutes before being poured into the mould, to ensure the powders can be dispersed uniformly throughout the polymer matrix. The mixture was then cured for 24 hours in a desiccator to ensure complete solidification occurred. The process was repeated for the remaining compositions, including 10%, 20%, 30%, 40%, 50%, and 60%, to create layers with varying properties. After the first layer had solidified, fabrication of the second layer continued by preparing a 100% PDMS layer. At this stage, the 100% PDMS

Table 1. The composition (%) of tin powder in the composite.

Filler/Matrix	Composite Label	Filler Composition (%)		Composite Overview
		Layer 1	Layer 2	
PDMS	Control	0		
Pure Tin	PS1	0	10	
	PS2	0	20	
	PS3	0	30	
	PS4	0	40	
	PS5	0	50	
	PS6	0	60	
Tin Alloy	AS1	0	10	
	AS2	0	20	
	AS3	0	30	
	AS4	0	40	
	AS5	0	50	
	AS6	0	60	
Pure Tin-Tin Alloy	TM1	10	10	
	TM2	20	20	
	TM3	30	30	
	TM4	40	40	
	TM5	50	50	
	TM6	60	60	

liquid polymer was poured on top of the cured mixed monolayer, maintaining the same thickness, and then subjected to the same curing procedure described previously.

A multilayer composite sample with dimensions of 2.0 cm × 2.0 cm × 0.5 cm was fabricated at the UiTM Cawangan Pulau Pinang using the layering technique. Each composite consisted of two layers, approximately 0.25 cm thick per layer. Layer 2 was prepared by mixing tin powder with PDMS polymer in specific composition ratios, as shown in Table 1. For the PS and AS series, Layer 1 was fabricated using 100% PDMS to provide a pure polymer surface, whereas for the TM series, both Layer 1 and Layer 2 were prepared using tin–PDMS mixtures to achieve higher filler loading and improved shielding characteristics. This design enabled comparison between composites with a pure polymer outer surface and those with fully metal–polymer integrated layers, providing insights into the influence of layering configuration on radiation attenuation.

Sample analysis

Density

According to the International Electrotechnical Commission (IEC), density (ρ) is the minimum mass per unit area of the protection material. Higher-density materials generally offer superior shielding capabilities due to more atoms per unit volume, which interact with and attenuate the radiation. Density is typically measured in grams per cubic centimeter (g/cm^3) as shown in Eqs. (2.1) and (2.2) below.[24]

$$\rho = \frac{\boldsymbol{mass}}{\boldsymbol{Volume}} \tag{2.1}$$

For a multilayer composite, an effective density can be measured using Eqs. (2.2) and (2.3)

$$\rho_{eff} = \frac{\boldsymbol{total\ mass}}{\boldsymbol{A}\ (t_1 + t_2)} \tag{2.2}$$

$$\rho_{eff} = \frac{\rho_1 t_1 + \rho_2 t_2}{t_1 t_2} \tag{2.3}$$

Where,

A = cross-sectional area of composite
ρ_{eff} = effective density
ρ_1 = density of the first layer composite
t_1 = the thickness of the first-layer composite
ρ_2 = density of the second-layer composite
t_2 = thickness of the second-layer composite

The difference in density was further calculated in percentage, called the percentage difference, as shown in Eq. (2.4).

$$\boldsymbol{Percentage\ difference} = \left| \frac{\boldsymbol{theoretical\ density} - \boldsymbol{calculated\ density}}{\boldsymbol{theoretical\ density}} \right| \times 100\% \tag{2.4}$$

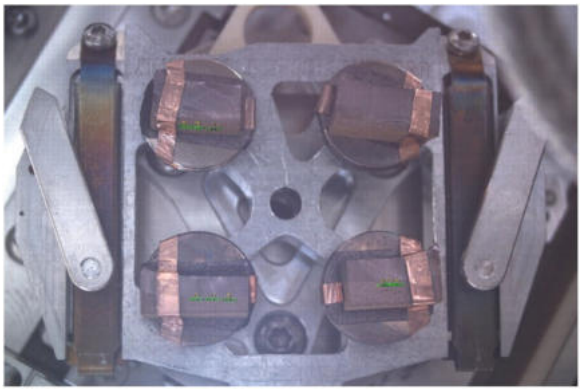

Fig. 1. Gold-coated composite with copper tape in FESEM.

The percentage difference in density depicts uniformity and consistency in the composite structure. A low value indicates a well-controlled fabrication process, as implied by the dispersion of tin particles. The disparities in the calculated densities are also due to cavities or uneven composite layers.[25] Thus, the calculated density should be as close as possible to its theoretical density for optimal performance and to ensure the homogeneity of the composites.[26–29]

Field emission scanning electron microscopy (FESEM - EDX)

Using an FEI Verios 460L, energy-dispersive X-ray spectroscopy (EDX) and field emission scanning electron microscopy (FESEM) were carried out at the SERC, USM facility. EDX determined the elemental composition and measured the oxygen concentration to assess potential microstructural defects. FESEM offered high-resolution images to study the topography and nanoscale characteristics of each sample. Samples were coated with a gold layer approximately 10 nm thick using a sputter coater. The FESEM-EDX analysis was performed at an accelerating voltage of 15 kV and a beam current of 1.6 nA, which provided adequate surface resolution and minimized charging. The samples were gold-coated and then fixed to stubs with colloidal copper tape, as shown in Fig. 1. A thorough understanding of material properties is made possible by FESEM 3D imaging capabilities and the ability to examine the nanoscale features of the Tin-PDMS composite.

Average porosity analysis

Porosity analysis was performed using ImageJ software. FESEM micrographs of the composites were imported, and the scale was calibrated using the embedded scale bars: 100 μm at 500x magnification and 50 μm at 1000x magnification. The thresholding function in ImageJ was applied to differentiate pores from the matrix, as demonstrated in Fig. 2. Once the threshold was adjusted and the region of interest was defined, ImageJ calculated the porosity area fraction, which was then expressed as relative porosity percentages. Using two magnifications ensured that the measurements captured both larger features and finer structural details, while maintaining accuracy in physical dimension calibration and minimizing pixel resolution bias. Porosity is a critical factor in the ability of multilayer composites, as it is affected by mechanical strength, conductivity, as well as durability.[30] This includes segmenting thresholding domains in the greyscale FESEM images that differentiate between voids and the material matrix, followed by the overall void area, and translating the results into the percentage area of the analyzed region[31] in an 8-bit-sized image.

Fourier transform infrared (FTIR) spectroscopy

Fourier Transform Infrared (FTIR) spectroscopy was carried out using a PerkinElmer Spectrum 100 series at Universiti Putra Malaysia (UPM), with spectra recorded in the wavenumber range of 3997–478 cm^1 at room temperature. This technique measures the absorption of infrared light by molecular vibrations, providing information on chemical bonding, functional groups, and interfacial stability of the materials. The equipment used for this characterization is shown in Fig. 3. FTIR was employed to examine the structural characteristics of control PDMS and its modified composites (PS1, AS1, and TM1). The resulting spectra display transmittance profiles that act as chemical fingerprints, enabling the identification of functional groups and the detection of changes due to compositional modifications.

Results and discussion

Density and percentage difference

Table 2 and Fig. 4 show the calculated densities of the PS, AS, and TM series composites. In all cases, density increased with tin content, consistent with the higher atomic density of the filler. The TM series achieved the highest effective density (up to 5.32 g/cm^3 at 60 wt.% tin), reflecting enhanced packing and reduced voids. This makes TM composites suitable for applications requiring structural rigidity and high load-bearing capacity. In contrast, PS composites exhibited lower densities and lighter weights, offering advantages for flexible or portable shielding designs. The AS series fell between these extremes,

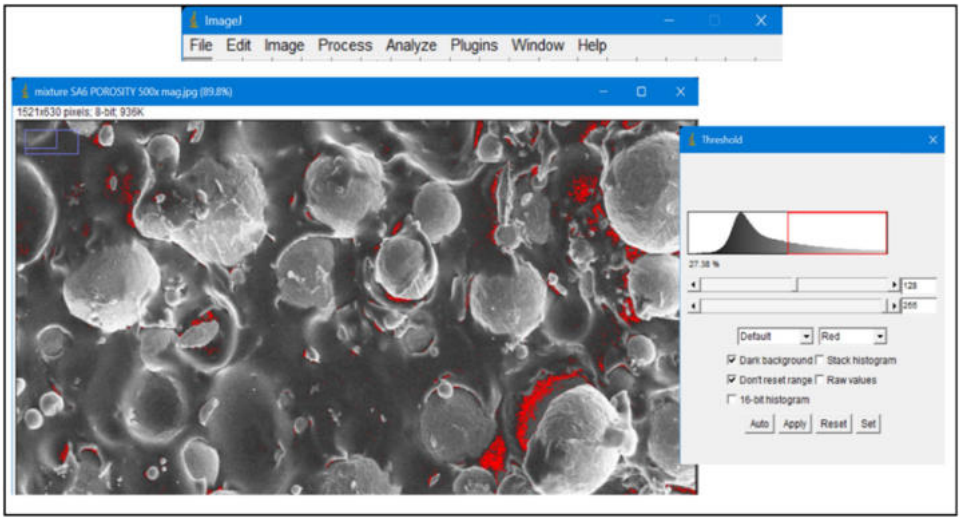

Fig. 2. Representative screenshot from ImageJ software showing the threshold adjustment for porosity region analysis of the PS1 composite (layer 2). The FESEM image was acquired at 500x magnification with a 100 μm scale bar.

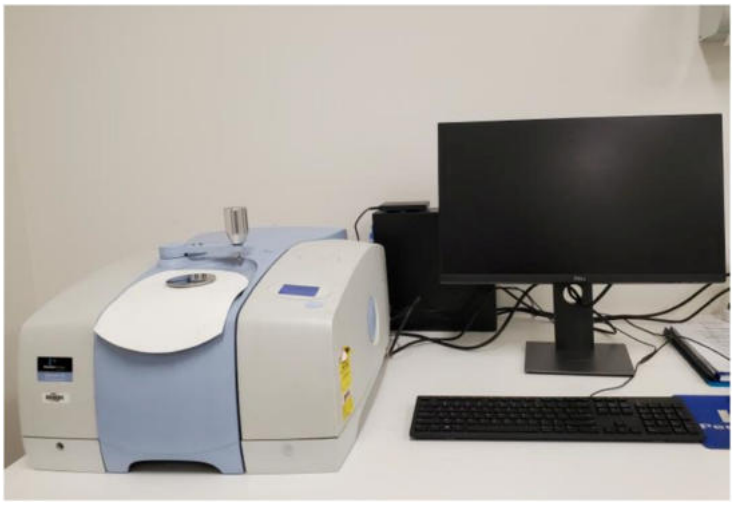

Fig. 3. Fourier Transform Infrared (FTIR) spectroscopy, conducted at Universiti Putra Malaysia (UPM) with the facility brand PerkinElmer, model Spectrum 100 series.

with intermediate densities and improved structural stability.

Percentage differences between theoretical and measured densities highlight the effects of porosity, filler distribution, and processing consistency.[32,33] For example, AS1 exhibited a high deviation (16.52%), while AS4 showed a much lower deviation (5.62%). The TM series generally displayed minimal variation ($<2\%$ for TM2–TM6), indicating more uniform filler distribution and fewer voids. These results emphasize the importance of controlled processing to achieve reliable density and structural performance.

Representative FESEM micrographs at 500x magnification are shown in Fig. 5. At low tin loadings (10–30 wt.%), the PS series exhibited relatively homogeneous particle dispersion. However, at higher loadings (40–60 wt.%), significant agglomeration occurred due to insufficient PDMS matrix to coat the filler particles, leading to voids and potential weakening of the composite.

The AS series displayed improved filler dispersion compared to the PS series, with alloy particles showing more spherical morphology and enhanced interfacial compatibility. This reduced agglomeration and promoted better adhesion between filler and matrix. In the TM series, the combination of pure tin and alloy fillers yielded a high packing density and enhanced bonding performance, effectively reducing void formation and delamination. Overall, FESEM analysis confirmed that filler morphology and dispersion strongly influence composite porosity and interfacial integrity.

Table 2. Calculated density values for multilayered tin-PDMS composite.

Composite Label	Mass (g)	Measured Thickness (cm)		Effective Density (g/cm^3)	Theoretical density (g/cm^3)	Percentage difference (%)
		Layer 1	Layer 2			
Control	2.00	0.52		0.962	1.103	12.78
PS1	2.78	0.25	0.26	1.36	1.41	3.54
PS2	2.63	0.23	0.25	1.37	1.72	20.53
PS3	3.58	0.24	0.25	1.83	2.03	10.20
PS4	3.59	0.21	0.25	1.95	2.34	16.78
PS5	4.95	0.28	0.25	2.34	2.66	12.05
PS6	5.16	0.22	0.19	3.15	2.97	6.11
AS1	2.85	0.45	0.13	1.24	1.49	16.52
AS2	4.51	0.33	0.13	1.45	1.87	22.35
AS3	6.25	0.20	0.38	2.32	2.26	2.90
AS4	5.89	0.16	0.34	2.79	2.64	5.62
AS5	8.00	0.18	0.33	3.11	3.03	2.77
AS6	10.21	0.22	0.36	3.42	3.41	0.07
TM1	2.49	0.31	0.14	1.77	1.80	1.57
TM2	3.20	0.31	0.23	2.47	2.49	0.90
TM3	4.25	0.20	0.32	3.24	3.19	1.61
TM4	5.27	0.12	0.20	3.96	3.88	1.91
TM5	4.96	0.18	0.33	4.69	4.58	2.40
TM6	6.54	0.20	0.25	5.32	5.27	0.94

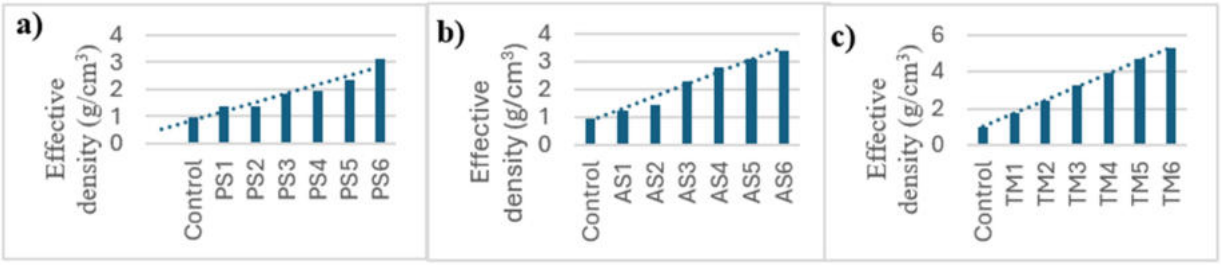

Fig. 4. Graph of calculated effective density of a) PS series, b) AS series, and c) TM series.

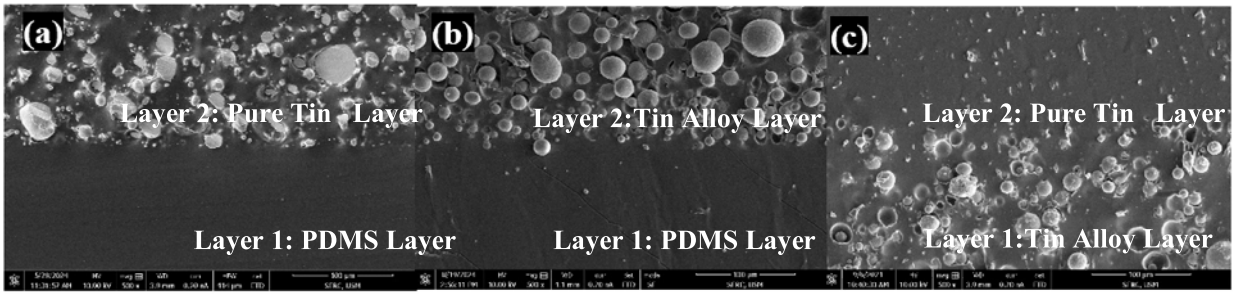

Fig. 5. FESEM images at 500x magnification of a) PS2, b) AS2, and c) TM2.

Elemental analysis using energy-dispersive X-ray spectroscopy (EDX)

Oxygen content trends, summarized in Table 3 and Fig. 6, further support the FESEM observations. The control PDMS sample showed the highest oxygen content (31.22 wt.%), originating from Si–O–Si linkages. However, at higher tin concentrations, a slight increase in oxygen content may occur due to the formation of SnO or SnO_2 as a result of oxidation.[33] Increasing tin content progressively reduced oxygen levels, as less polymer was present. For example, oxygen decreased from 26.59 wt.% in PS1 to 18.26 wt.% in PS6.

At higher tin loadings (>50 wt.%), oxygen content slightly increased, attributed to the formation of SnO/SnO_2 due to surface oxidation of tin particles. This was most evident in AS5–AS6 and the TM series, where oxygen levels remained in the 19–28 wt.% range. While tin oxides may enhance radiation attenuation due to their high atomic number, excessive oxidation can reduce flexibility and compromise long-term durability. Thus, minimizing uncontrolled oxidation during fabrication is essential

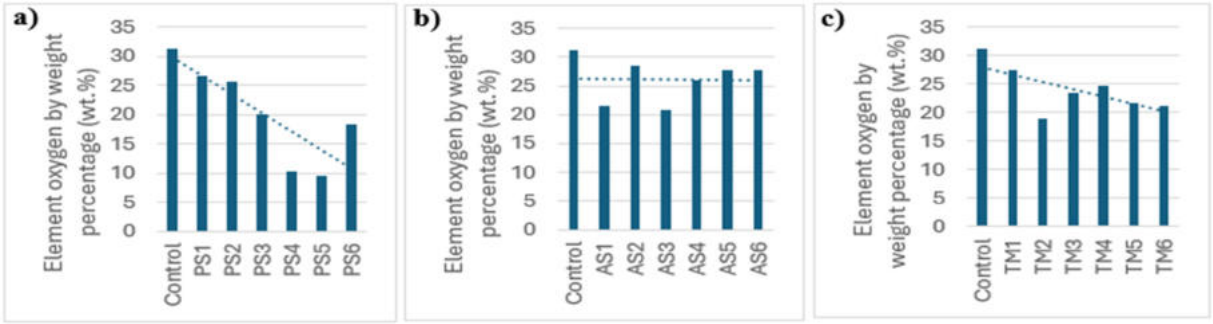

Fig. 6. Element oxygen weight percentage against tin composition in a) PS series, b) AS series, and c) TM series.

for ensuring structural reliability. These oxides appear because of enhanced interaction between the tin concentration and the oxygen present in the environment or the composite matrix.[34] The composite has a large surface area of tin particles, which may also encourage further oxidation at this point, which would reintroduce oxygen in the form of tin oxides and account for the composition's rapid increase in oxygen percentage.[34]

Oxygen has been associated with composite oxidation. The presence of oxygen can have a positive or negative coefficient depending on the composition of the material and conditions. Nevertheless, oxidation can enhance certain properties like radiation shielding, as in the case of high atomic number oxides like tin oxide, because it brings oxygen into the structure, but in many cases, it degrades the performance of radiation-shielding composites.[35] Oxygen can also cause the polymer matrix, leading to chain scission, embrittlement, or lowered ductility. These effects damage the matrix structure, reducing the composite's efficiency in radiation attenuation. The formation of oxides that involve oxygen might be responsible for the nonuniformity of the composite. This unevenness can lead to the formation of 'leaky points', which decrease the ability to shield.[36,37] They may degrade faster in radiation-net environments such as space or nuclear power plants in synergistic effects of radiation, oxygen, and weather factors like temperature and humidity.

Table 3. Element oxygen by weight percentage.

Composite Label	Element oxygen by weight percentage (wt.%)
Control	31.22
PS1	26.59
PS2	25.68
PS3	20.04
PS4	10.37
PS5	9.56
PS6	18.26
AS1	21.57
AS2	28.52
AS3	20.79
AS4	26.13
AS5	27.79
AS6	27.65
TM1	27.48
TM2	19.02
TM3	23.51
TM4	24.57
TM5	21.58
TM6	21.22

Average porosity analysis

Fig. 7 presents the porosity region of the PS1 composite for layer 2, analyzed using ImageJ software. The image was obtained at 500x magnification with a scale bar of 100 μm, which was applied to calibrate the region size during analysis. This calibration ensures that the porosity measurements reflect the true physical dimensions of the sample rather than only pixel counts. FESEM images at both 500x and 1000x magnifications were utilized to obtain reliable measurements across different areas of the sample. The average porosity values were calculated as relative porosity percentages. Results indicate that the PS series shows very low porosity in layer 1 (ranging from 0% to 0.01% within the PDMS layer) and slightly higher values in layer 2 (associated with the pure tin mixture). Nevertheless, overall porosity remains minimal, and major line porosity is consistently low in both layers, suggesting that the fabrication process achieved good structural resistance and reduced the likelihood of void formation.

The variability of porosity percent in PS series, AS series, and TM series composites based on layer content is highlighted in relative percentage trends as shown in Fig. 7, reflective of Table 4. In the AS series, for layer 1 (PDMS layer), all the composites reveal negligible porosity, ranging from 0% to 0.07%. However, for layer 2 (tin alloy mixture), all composites except AS1 and AS2 show a much higher porosity. Total porosity values in the AS series range from 0.21 % to 0.67 %, and due to the predominance of porosity in the second layer, the problem of uniform packing

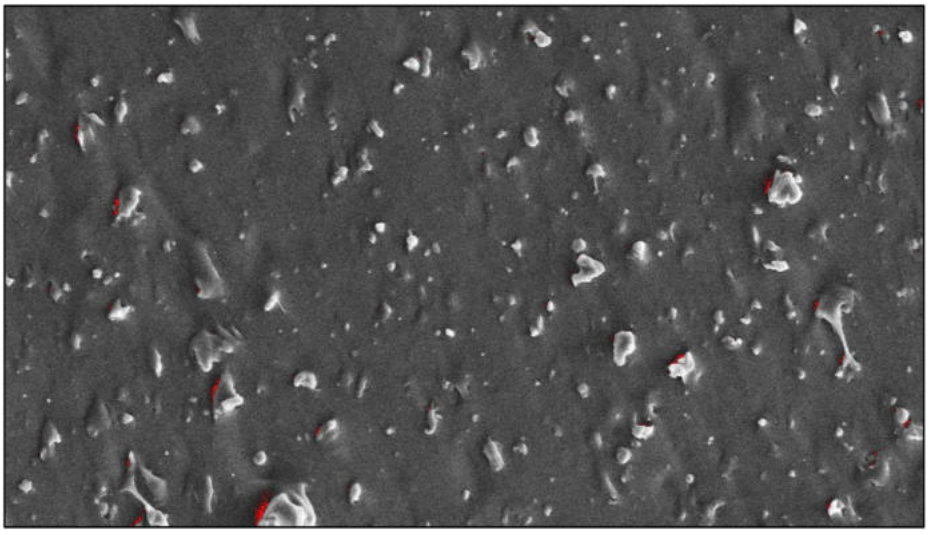

Fig. 7. Porosity region in the PS1 composite measured for layer 2 using ImageJ software analysis. The FESEM image was acquired at 500x magnification with a 100 μm scale bar, which was used for calibration of the analyzed region.

Table 4. The porosity percentage of each composite.

	Effective porosity (%)		
Composite Label	Layer 1	Layer 2	Total
PS1	0.01	0.08	0.09
PS2	0.00	0.13	0.13
PS3	0.00	0.01	0.01
PS4	0.01	0.03	0.03
PS5	0.00	0.01	0.01
PS6	0.07	0.09	0.16
AS1	0.00	0.65	0.65
AS2	0.07	0.60	0.67
AS3	0.02	0.19	0.21
AS4	0.00	0.41	0.41
AS5	0.01	0.33	0.34
AS6	0.01	0.22	0.23
TM1	0.12	0.12	0.24
TM2	0.09	0.10	0.19
TM3	0.08	0.17	0.25
TM4	0.10	0.20	0.30
TM5	0.13	0.53	0.66
TM6	0.58	0.58	1.16

or perfect bonding between the tin alloy and polymer matrix can be assumed. This trend simply suggests the general need for enhanced processing techniques to ensure that porosity is well-controlled and that the structural loading property of AS composites is well-augmented.

Porosity analysis using ImageJ confirmed that void formation primarily occurred in the filler-rich layers (Table 4, Fig. 8). In the PS series, porosity remained very low (0.01–0.16%), indicating consistent microstructural integrity. The AS series exhibited higher porosity (0.21–0.67%), especially in the filler layer, suggesting incomplete packing or bonding at higher alloy contents. The TM series showed the highest porosity (0.24–1.16%), consistent with its dual filler design. For instance, TM6 exhibited 1.16% porosity, significantly higher than PS or AS composites. Nevertheless, TM composites compensated with higher density and improved bonding due to the synergistic effects of alloy and pure tin fillers. These results highlight that porosity is strongly linked to fabrication conditions and filler interactions, with direct implications for density and mechanical stability.

Fourier transform infrared (FTIR) spectroscopy

FTIR spectra of control PDMS, PS1, AS1, and TM1 are shown in Fig. 9. Control PDMS exhibited the expected peaks: Si–O–Si stretching (1000–1100 cm^1), C–H stretching (2960–2850 cm^1), and Si–C vibrations (~800 cm^1). These confirmed the siloxane backbone of the matrix. For the control PDMS spectrum, the expected characteristic peaks of polydimethylsiloxane are observed. The strong absorption between 1000 and 1100 cm^1 corresponds to Si–O–Si stretching, confirming the siloxane backbone of PDMS. Peaks in the range of 2960–2850 cm^1 indicate C–H stretching from methyl groups, while a distinct signal around 800 cm^1 reflects Si–C vibrations. These are typical and confirm the identity of unmodified PDMS.[38] Composite spectra retained these backbone features, indicating chemical compatibility between PDMS and tin fillers. However, subtle differences were observed: PS1 showed weak carbonyl absorption (~1700 cm^1), AS1 exhibited a broader O–H band (~3300 cm^1), and TM1 displayed complex signals in the fingerprint region (<1000 cm^1), suggesting filler–matrix interactions and potential surface functionalization. The overall reduction in transmittance with increasing tin content reflects enhanced scattering and absorption

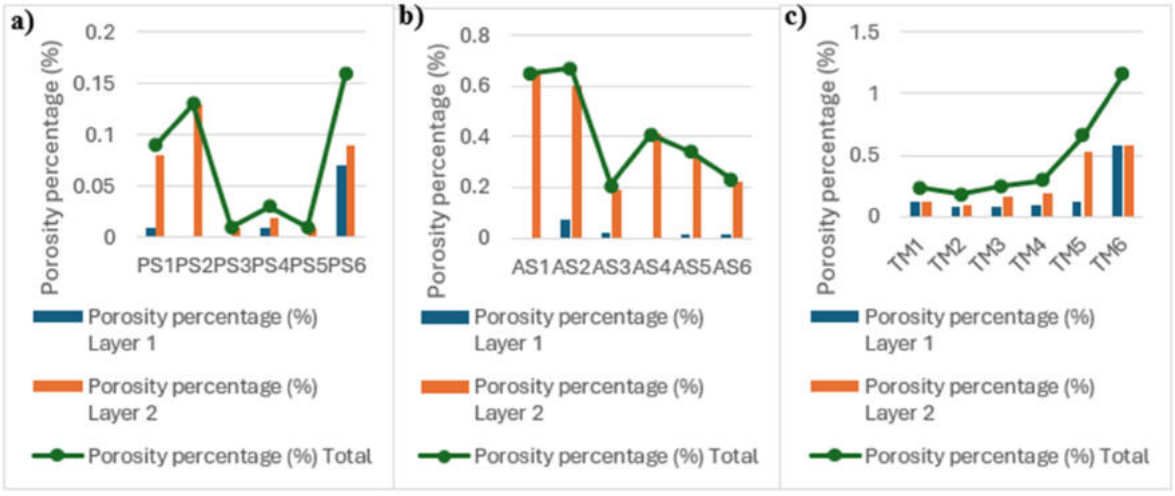

Fig. 8. Porosity percentage of each layer and total percentage for a) PS series, b) AS series, and c) TM series.

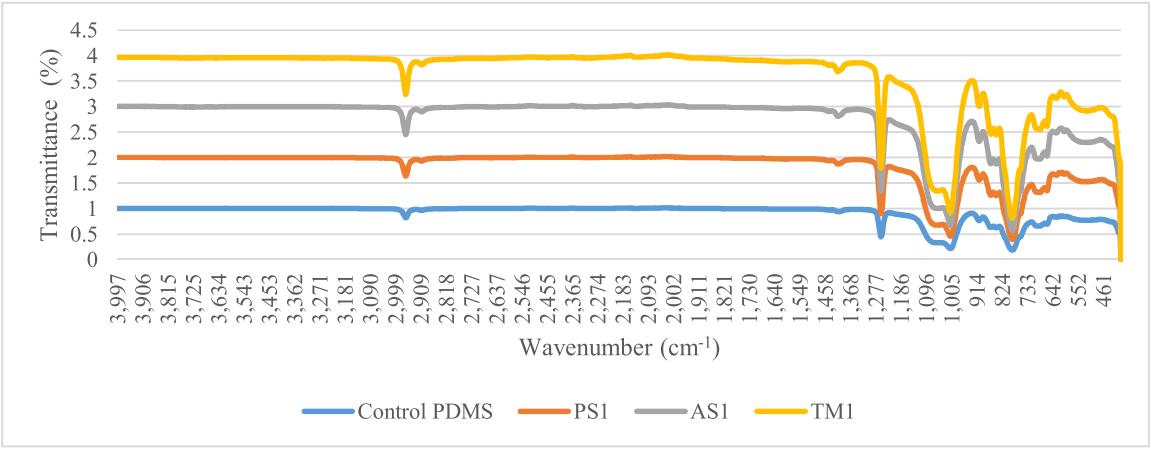

Fig. 9. FTIR spectrum of the Control, PS1, AS1, and TM1 composite.

Table 5. Summary data of conventional lead and best morphological samples.

Samples	Density (g/cm^3)	Porosity (%)	Notes on Radiation Attenuation
Lead	11.34	–	High density; absorbs more radiation
AS5	3.11	0.34	Balanced density and structure; flexible
TM6	5.32	1.16	High density, suitable for flexible shielding

by metallic fillers. The degree of transmittance reduces as the tin content increases, which suggests greater scattering and absorption from the fillers incorporated.[38]

Result summary

Table 5 compares the density and porosity of conventional lead with the best-performing tin–PDMS composites. Lead remains the densest material, 11.34 g/cm^3,[39] offering superior shielding but with drawbacks in terms of brittleness, toxicity, and weight. Among the composites, AS5 (3.11 g/cm^3, 0.34% porosity) demonstrated the best balance between density, low porosity, and flexibility, making it a reliable candidate for structural shielding applications. TM6 (5.32 g/cm^3, 1.16% porosity), while slightly more porous, achieved the highest effective density among the composites, positioning it as the closest morphological match to lead. These findings highlight that although tin–PDMS composites do not yet match the shielding density of lead, they provide significant advantages in flexibility, processability, and safety, making them promising alternatives for specific radiation protection applications.

Conclusion

The PS, AS, and TM composite series demonstrated distinct structure-property relationships. Density increased with tin content, with the TM6 composite achieving the highest effective density (5.32 g/cm^3). FESEM and porosity analysis confirmed that filler dispersion critically affects microstructural integrity, with PS composites showing the lowest porosity, AS composites achieving improved interfacial adhesion, and TM composites balancing density with bonding performance.

EDX results revealed decreasing oxygen content with higher tin loading, though surface oxidation introduced secondary effects. FTIR confirmed that filler incorporation did not disrupt the PDMS backbone but induced subtle modifications in functional groups.

Overall, AS5 (3.11 g/cm^3, 0.34% porosity) emerged as the most balanced composite, combining low porosity with satisfactory density and structural stability, while TM6 (5.32 g/cm^3, 1.16% porosity) provided the highest effective density, offering the closest morphological comparison to conventional lead.

While lead (11.34 g/cm^3) remains unmatched in density and attenuation, the developed tin–PDMS composites demonstrate clear advantages in terms of flexibility, safety, and lightweight performance. These results establish a strong microstructural foundation for future comparative studies with lead-based shields and underline the potential of tin–PDMS composites as safer, lead-free alternatives for radiation protection applications.

While the developed tin–PDMS double-layer composites demonstrated promising density, porosity, and morphological characteristics, some limitations should also be considered. The double-layer structure, while enhancing shielding capability, may influence long-term stability due to potential interlayer adhesion issues, particularly under repeated bending, cyclic mechanical loading, or thermal stress. FESEM cross-sectional images at higher tin loadings suggested localized regions prone to delamination, which may compromise flexibility and durability. In addition, the relatively high porosity observed in some TM composites highlights the need for tighter control of fabrication conditions to avoid void formation. To overcome these challenges, future research should focus on optimizing layer thicknesses to achieve a balance between shielding efficiency and flexibility, scaling up the layer-by-layer curing process to ensure reproducibility in larger-scale applications. Long-term performance testing, including accelerated aging and mechanical fatigue studies, is also necessary to evaluate the durability of these composites under real-world conditions.

Acknowledgment

The authors would like to thank Universiti Teknologi MARA Cawangan Pulau Pinang, Universiti Putra Malaysia, and Universiti Sains Malaysia for their contributions, support, and the provision of access to workstation facilities.

Authors' declaration

- Conflicts of Interest: None.
- We hereby confirm that all the Figures and Tables in the manuscript are mine/ours. Furthermore, any Figures and images that are not mine/ours have been included with the necessary permission for republication, which is attached to the manuscript.
- No animal studies are present in the manuscript.
- No human studies are present in the manuscript.
- Ethical Clearance: The project was approved by the local ethical committee at Universiti Teknologi MARA Cawangan Pulau Pinang, 13500 Permatang Pauh, Pulau Pinang, Malaysia.

Authors' contributions statement

N. S. R. and N. M. A. M. were responsible for writing the original draft and editing the manuscript. N. S. R. and H. Z. A. contributed to the data collection. Data analysis was carried out by N. S. R., A. Z. S., H. Z. A., and N. I. N. I. The manuscript was revised and supervised by N. M. A. M., A. M., N. A. A. W., and R. Z. All authors have read and approved the final version of the manuscript.

Funding statements

The authors would like to acknowledge the Ministry of Higher Education (MOHE) for the financial support provided through the Fundamental Research Grant Scheme (FRGS/1/2023/STG05/UITM/03/3).

References

1. Aldhuhaibat MJR, Amana MS, Jubier NJ, Salim AA. Improved gamma radiation shielding traits of epoxy composites: Evaluation of mass attenuation coefficient, effective atomic and electron number. Radiation Physics and Chemistry. 2021;179. https://doi.org/10.1016/j.radphyschem.2020.109183.
2. Miranda I, Souza A, Sousa P, *et al.* Properties and Applications of PDMS for Biomedical Engineering: A Review. J Funct Biomater. 2021;13(1):2. https://doi.org/10.3390/jfb13010002.
3. AbuAlRoos NJ, Baharul Amin NA, Zainon R. Conventional and new lead-free radiation shielding materials for

radiation protection in nuclear medicine: A review. Radiation Physics and Chemistry. 2019;165:108439. https://doi.org/10.1016/J.RADPHYSCHEM.2019.108439.
4. Azman MN, Abualroos NJ, Yaacob KA, Zainon R. Feasibility of nanomaterial tungsten carbide as lead-free nanomaterial-based radiation shielding. Radiation Physics and Chemistry. 2023;202:110492. https://doi.org/10.1016/J.RADPHYSCHEM.2022.110492.
5. El-Khatib AM, Zard K, Abbas MI, Gouda MM. Novel composite based on silicone rubber and a nano mixture of SnO_2, Bi_2O_3, and CdO for gamma radiation protection. Sci Rep. 2024;14(1). https://doi.org/10.1038/s41598-024-51965-0.
6. Boice J, Dauer LT, Kase KR, Mettler FA, Vetter RJ. Evolution of radiation protection for medical workers. Br J Radiol. 2020;93(1112). https://doi.org/10.1259/bjr.20200282.
7. Martínez-Farías FJ, Alvarado-Sánchez A, Rodríguez-Rojas EO. Methodology for inspecting the functional state of radiological protection accessories for use in Radiodiagnosis. Clinical innovations in health research-HJM. 2024;1(3). https://doi.org/10.24875/CIHR.24000008.
8. Behzadmehr R, Doostkami M, Sarchahi Z, Dinparast Saleh L, Behzadmehr R. Radiation protection among health care workers: knowledge, attitude, practice, and clinical recommendations: a systematic review. Rev Environ Health. 2021;36(2):223–234. https://doi.org/10.1515/reveh-2020-0063.
9. Glaser M, Matthes S, Hildebrand J, Pierre Bergmann J, Schaaf P. Hybrid Thermoplastic-Metal joining based on Al/Ni multilayer foils — Analysis of the joining zone. Mater Des. 2023;226:111561. https://doi.org/10.1016/j.matdes.2022.111561.
10. Libeesh NK, Naseer KA, Mahmoud KA, *et al.* Applicability of the multispectral remote sensing on determining the natural rock complexes distribution and their evaluability on the radiation protection applications. Radiation Physics and Chemistry. 2022;193:110004. https://doi.org/10.1016/j.radphyschem.2022.110004.
11. Kamarolzeman JA, AM NM. A Review on the personal protective equipment (PPE) used in occupational radiation protective. Virtual Science Invention Innovation Conference (SIIC). 2020;(9):299–300. Accessed December 31, 2024.
12. Jung J, Yoon S, Kim B, Kim JB. Development of High-Performance Flexible Radiative Cooling Film Using PDMS/TiO_2 Microparticles. Micromachines (Basel). 2023;14(12). https://doi.org/10.3390/mi14122223.
13. Shaker DS, Abass NK, Ulwall RA. Preparation and study of the structural, morphological and optical properties of pure tin oxide nanoparticle doped with Cu. Baghdad Science Journal. 2022;19(3):660–669. https://doi.org/10.21123/BSJ.2022.19.3.0660.
14. Gilys L, Griškonis E, Griškevicius P, Adliene D. Lead Free Multilayered Polymer Composites for Radiation Shielding. Polymers (Basel). 2022;14(9):1696. https://doi.org/10.3390/polym14091696.
15. Almuqrin AH, Sayyed MI, Alorain DA, Elsafi M. Multilayer radiation shields for nuclear and radiological centers using free-lead materials and nanoparticles. Ann Nucl Energy. 2024;200:110404. https://doi.org/10.1016/J.ANUCENE.2024.110404.
16. Nakamura K, Kubo K, Hirata M, *et al.* Evaluation of the shielding effectiveness of a non-toxic, double-layered $BaSO_4$/W composite against diagnostic X-rays. Radiation Physics and Chemistry. 2024;219. https://doi.org/10.1016/j.radphyschem.2024.111684.
17. Chen Z, Li X, Lu L, *et al.* Non-Toxic and Flexible Radiation-Shielding Composites Based on Natural Rubber Containing Elemental W Fillers for Efficient Shielding against X/γ-rays. Processes. 2023;11(3):674. https://doi.org/10.3390/pr11030674.
18. Ahmed B, Shah GB, Malik AH, Aurangzeb, Rizwan M. Gamma-ray shielding characteristics of flexible silicone tungsten composites. Applied Radiation and Isotopes. 2020;155. https://doi.org/10.1016/j.apradiso.2019.108901.
19. Mhareb MHA, Alajerami YSM, Sayyed MI, *et al.* Radiation shielding, structural, physical, and optical properties for a series of borosilicate glass. J Non Cryst Solids. 2020;550:120360. https://doi.org/10.1016/j.jnoncrysol.2020.120360.
20. Jayakumar S, Saravanan T, Philip J. A review on polymer nanocomposites as lead-free materials for diagnostic X-ray shielding: Recent advances, challenges and future perspectives. Hybrid Advances. 2023;4:100100. https://doi.org/10.1016/j.hybadv.2023.100100.
21. Nagaraja N, Manjunatha HC, Seenappa L, Sridhar KN, Ramalingam HB. Radiation shielding properties of silicon polymers. Radiation Physics and Chemistry. 2020;171:108723. https://doi.org/10.1016/j.radphyschem.2020.108723.
22. Wang X, Zhao L, Fuh JYH, Lee HP. Effect of porosity on mechanical properties of 3D printed polymers: Experiments and micromechanical modeling based on X-ray computed tomography analysis. Polymers (Basel). 2019;11(7). https://doi.org/10.3390/polym11071154.
23. Xuan W, Fang Y, Teng S, *et al.* In situ fabrication of porous polymer films embedded with perovskite nanocrystals for flexible superhydrophobic piezoresistive sensors. J Colloid Interface Sci. 2024;669:358–365. https://doi.org/10.1016/j.jcis.2024.04.140.
24. Agarwal BD, Broutman LJ, Chandrashekhara K. Analysis and Performance of Fiber Composites Third Edition; 2006.
25. Kim SC. Metal Particle Pencil Beam Spray-Coating Method for High-Density Polymer–Resin Composites: Evaluation of Radiation-Shielding Sheet Properties. Materials. 2023;16(18). https://doi.org/10.3390/ma16186092.
26. Abualroos NJ, Idris MI, Ibrahim H, Kamaruzaman MI, Zainon R. Physical, mechanical, and microstructural characterisation of tungsten carbide-based polymeric composites for radiation shielding application. Sci Rep. 2024;14(1):1375. https://doi.org/10.1038/s41598-023-49842-3.
27. Yilmaz SN, Güngör A, Özdemir T. The investigations of mechanical, thermal and rheological properties of polydimethylsiloxane/bismuth (III) oxide composite for X/Gamma ray shielding. Radiation Physics and Chemistry. 2020;170:108649. https://doi.org/10.1016/j.radphyschem.2019.108649.
28. Izdihar K, Abdul Razak HR, Supion N, Karim MKA, Osman NH, Norkhairunnisa M. Structural, Mechanical, and Dielectric Properties of Polydimethylsiloxane and Silicone Elastomer for the Fabrication of Clinical-Grade Kidney Phantom. Applied Sciences. 2021;11(3):1172. https://doi.org/10.3390/app11031172.
29. Dejangah M, Ghojavand M, Poursalehi R, Gholipour PR. X-ray attenuation and mechanical properties of tungsten-silicone rubber nanocomposites. Mater Res Express. 2019;6(8):085045. https://doi.org/10.1088/2053-1591/ab1a89.
30. Zhang Y, Li WY, Lan R, Wang JY. Quality Monitoring of Porous Zein Scaffolds: A Novel Biomaterial. Engineering. 2017;3(1):130–135. https://doi.org/10.1016/J.ENG.2017.01.001.
31. Wang B, Qiu T, Yuan L, *et al.* A comparative study between pure bismuth/tungsten and the bismuth tungsten

oxide for flexible shielding of gamma/X rays. Radiation Physics and Chemistry. 2023;208. https://doi.org/10.1016/j.radphyschem.2023.110906.
32. Roslan NS, Mukhtar NMA, Abidin HZ, *et al.* Radiation Shielding Performance of Double-Layered Tin-PDMS Against 661.7 keV Gamma Rays. International Journal of Innovation and Industrial Revolution (IJIREV). 2025;7(22).
33. Zainal Abidin H, Mukhtar NMA, Mahmood A, *et al.* Effect of tin filler composition on porosity in tin-polydimethylsiloxane composites. Pure and Applied Chemistry. 2025;97(8):825–840. https://doi.org/10.1515/pac-2024-0347.
34. Chen Z, Wang C, Li J, Song F, Zhang Z. Conductor selection and economic analysis of D.R. congo–guinea ±800 kV UHVDC transmission project. Global Energy Interconnection. 2020;3(4):385–397. https://doi.org/10.1016/j.gloei.2020.10.007.
35. More CV, Alsayed Z, Badawi Mohamed S, Thabet Abouzeid A, Pawar PP. Polymeric composite materials for radiation shielding: a review. Environ Chem Lett. 2021;19(3):2057–2090. https://doi.org/10.1007/s10311-021-01189-9.
36. Li Y, Wu D, Zhang Y, Wang L, Xue S. Effects of trace oxygen content on microstructure and performances of Au-20Sn/Cu solder joints. Crystals (Basel). 2021;11(6). https://doi.org/10.3390/cryst11060601.
37. Martins JRS, Araújo RO, Donato TAG, Arana-Chavez VE, Buzalaf MAR, Grandini CR. Influence of oxygen content and microstructure on the mechanical properties and biocompatibility of Ti-15 wt%mo alloy used for biomedical application. Materials. 2014;7(1):232–243. https://doi.org/10.3390/ma7010232.
38. Zainal Abidin H, Mukhtar NMA, Mahmood A, Abdul Wahab NA, Zainon R, Roslan NS. Radiation Protection of Tin-Polydimethylsiloxane (PDMS) Composites Against Gamma Ray at 356 keV. International Journal of Innovation and Industrial Revolution. 2025;7(20):352–369. https://doi.org/10.35631/IJIREV.720023.
39. Gurumurthi SHP, Rajasekar V. Comparative Analysis of Effectiveness of Traditional Lead Aprons versus Newer Generation Lead-free Aprons in Radiation Protection. J Med Phys. 2025;50(1):1–7. https://doi.org/10.4103/jmp.jmp_152_24.

المركّبات المزدوجة الطبقات من القصدير وبولي دايميثيل سيلوكسان المسامية والمورفولوجيا البنيوية للمركّبات البوليمرية تقييم :(PDMS)

نورول شفيقة روسلان[1]، نور ميزاتول أزرا مختار[3،2،1]، أينورخيلة محمود[1]، نور أيمي عبد الوهاب[1]، رافيده زاينون[3]، حنيصة زينال عابدين[1]، عائشة زرزالي شاه[4]، نور إيواني نور إزهام[5]

[1]قسم العلوم التطبيقية، جامعة التكنولوجيا مارا، فرع بينانغ، 13500 برماتانغ باوه، ولاية بينانغ، ماليزيا.
[2]كلية العلوم الصحية، جامعة التكنولوجيا مارا، فرع بينانغ، 13200 كَبَلا باتاس، ولاية بينانغ، ماليزيا.
[3]قسم التصوير الطبي الحيوي، معهد الطب والأسنان المتقدّم، جامعة العلوم الماليزية، *SAINS@BERTAM*، 13200 كَبَلا باتاس، ولاية بينانغ، ماليزيا.
[4]مركز أساسيات*UiTM* ، جامعة التكنولوجيا مارا، فرع سيلانغور، حرم دنقفل، 43800 دنقفل، سيلانغور، ماليزيا.
[5]كلية العلوم التطبيقية، جامعة التكنولوجيا مارا شاه علم، 40450 شاه علم، سيلانغور، ماليزيا.

الملخص

إنّ السعي نحو تطوير مواد متقدمة للحماية من الإشعاع قد أبرز إمكانية استخدام المركّبات البوليمرية–المعدنية. وتُعدّ المسامية عاملاً رئيسياً يؤثر في قدرة المادة على إيقاف الإشعاع، إذ إن انخفاض عدد الفجوات يحدّ من مسارات الاختراق الإشعاعي. وتشير الدراسات الحديثة إلى أهمية توزيع الحشوة المعدنية في تعزيز الخصائص الميكانيكية وأداء الحماية. يستعرض هذا العمل المورفولوجيا البنيوية والمسامية لمركّبات القصدير PDMS–المُحضّرة باستخدام حشوات من القصدير النقي (PS) وسبائك القصدير (AS) بنسب تحميل تتراوح بين 10–60% وزناً، بالإضافة إلى سلسلة حشوات خليط القصدير .(TM) وقد جرى تحليل السمات المورفولوجية وتوزيع الجسيمات ومحتوى الأكسجين والمسامية بشكل شامل. أظهرت النتائج أن المسامية ترتبط ارتباطاً وثيقاً بتوزيع الحشوة وتركيبها. حيث أظهر المركّب (AS5بنسبة 50% وزناً من سبيكة القصدير) أفضل توازن في الخصائص، إذ حقق مسامية منخفضة بلغت 0.34% مع كثافة مناسبة واستقرار بنيوي جيد. وفي سلسلة TM، أظهر المركّب (TM6بنسبة 60% وزناً من خليط القصدير) خصائص واعدة لتطبيقات الحماية عالية الكثافة، وذلك بفضل محتواه العالي من القصدير وكثافته البالغة 5.32 غ/سم³ ومسامية أقل من 2.0% ضمن الحد المقبول للمركّب. تمثل هذه النتائج أساساً لفهم الخصائص الميكروية لمركّبات القصدير–PDMS كخطوة نحو تطوير مواد بديلة خالية من الرصاص للحماية الإشعاعية.

الكلمات المفتاحية: المركّبات مزدوجة الطبقات، برنامج ImageJ، البوليمرات–المعادن، المسامية، التدرّع الإشعاعي (الحماية من الإشعاع).